E-ISSN 2586-9027
Homepage : https://tci-thaijo.org/index.php/SciTechAsia Science & Technology Asia
Vol.30 No.2 April - June 2025 Page: [97-107]
Original research article

A Model for the Water Saturation Dependence of Electrical Conductivity of Porous Media

Luong Duy Thanh[1,*], Nguyen Manh Hung[1,2,3], Nguyen Van Nghia[1], Phan Van Do[1], Nguyen Tien Hung[4]

[1] *Thuyloi University, Hanoi 116705, Vietnam*
[2] *Graduate School, Phenikaa University, Hanoi 12116, Vietnam*
[3] *Phenikaa Institute for Advanced Study (PIAS), Phenikaa University, Hanoi 10000, Vietnam*
[4] *Institute of Earth Sciences, Vietnam Academy of Science and Technology, Hanoi 10000, Vietnam*

Received 1 January 2024; Received in revised form 22 May 2025
Accepted 4 June 2025; Available online 18 June 2025

ABSTRACT

Electrical conductivity (EC) measurement has been extensively applied for characterization of geological media on account of its high sensitivity to various parameters of water-filled porous media (i.e., structure, water content, water composition). It is one of most frequently used methods in geological, geotechnical, and environmental problems. Its effectiveness relies on theoretical models that relate the EC and parameters of porous media. In this work, we develop an EC model for porous media under partially saturated conditions using a bundle of capillary tubes model. The proposed model is expressed in terms of electrical conductivity of pore water, electrical surface conductivity, water saturation, microstructure parameters of porous media (e.g., porosity, tortuosity, minimum and maximum pore radii) and their pore size distribution. The model is then numerically analyzed and successfully compared with experimental data in literature and published models.

Keywords: Electrical conductivity; Porosity; Tortuousity; Porous media; Water saturation

1. Introduction

Over the past few decades, geophysical methods have been extensively applied to identify hydrological processes. Among the geophysical methods, the electrical and electro-magnetic methods, such as induced polarization, electrical resistivity tomography and electromagnetic induction, have received strong interest in oil/mineral exploration and environmental research since they can provide quantitative information on the structure, water content, or pore wa-

***Corresponding author:** thanh_lud@tlu.edu.vn **doi:** 10.14456/scitechasia.2025.28

ter composition of porous media through the EC measurement. For further details on such methods, we refer readers to published works [1, 2]. Those methods can be done fairly quickly with a simple setup for measurements. Because the methods are non-destructive and highly sensitive, they provide a very attractive tool for describing subsurface properties. Consequently, they have been applied in different areas such as groundwater investigation, landfill and solute transport delineation or agronomic management [3, 4].

Electrical conduction in water-filled porous media mostly happens through movement of ions in pore water. In addition, electrical conduction can happen in the vicinity of mineral surfaces in contact with water and that is characterized by the surface conductance (i.e., electrical surface conductivity). There exist many EC models for water-filled porous media in the literature [5–7]. Different approaches have been applied to develop EC models such as the effective medium, percolation theory or capillary tube model [8, 9]. Surface conductivity has also been considered in EC models [10–13]. Recently, there have been an increasing number of EC models based on the fractal nature of pores in porous media, that is the fractal pore size distribution (PSD) [14–18]. Besides the fractal PSD; there are also other PSDs such as lognormal PSD, double lognormal PSD, similarly skewed PSD (SSPSD) or realistic non-monotonic PSD directly obtained from measurements that can be applied to study transport phenomena in porous media [19–21]. Recently, Nghia and co-authors applied the SSPSD to develop a EC model under fully saturated conditions [22]. It is seen that the model is well capable of explaining published data. However, to the best of our knowledge, there has not yet been such a model using SSPSD under partially saturated conditions.

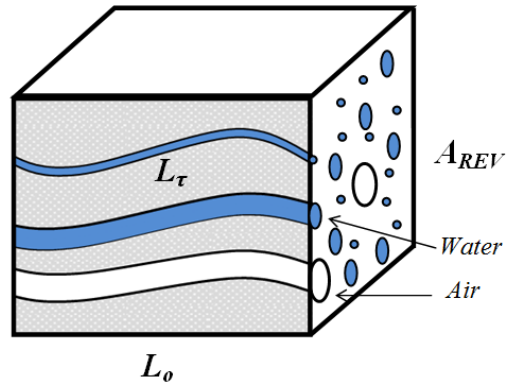

Fig. 1. Conceptual model of a porous medium as a bundle of capillaries [23]. At a given capillary pressure, the capillary is either filled by water or by air depending on its radius.

This work includes three sections. In section 2, we develop an EC model of porous media under partially saturated conditions using using a bundle of capillary tubes model with SSPSD. The obtained model is expressed in terms of electrical conductivity of pore water, electrical surface conductivity, effective water saturation, mirostructure parameters and the PSD of porous media. In section 3, the model is then numerically analyzed and compared with experimental data in literature and published models.

2. Model Development

The present model is an extension of the EC models proposed by [14, 22] for the case of partially saturated conditions. Therefore, the approach to develop the model is similar to those in [14, 22]. Firstly, we consider a representative elementary volume (REV) of porous media as a cube with the length of L_o (see Fig. 1). In the context of a bundle of capillary tubes model, the REV is conceptualized as

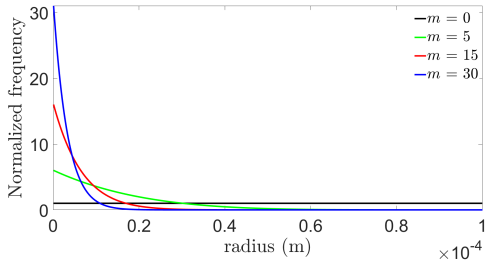

Fig. 2. Frequency distribution of pore radius following Eq. (2.1) between $r_{\min} = 10^{-7}$ m and $r_{\max} = 10^{-4}$ m, for example, for different values of the exponent m.

an equivalent bundle of capillary tubes with radii varying from a minimum pore radius $r_{\min}$ to a maximum pore radius $r_{\max}$. The PSD is such that the number of capillaries with radii between r and $r + \mathrm{d}r$ is given by $f(r)\mathrm{d}r$. For the SSPSD, the $f(r)$ is given by [19]:

$$f(r) = D\left(\frac{r - r_{\max}}{r_{\min} - r_{\max}}\right)^m, \qquad (2.1)$$

where D and m are constants that define the shape of the PSD. For $m = 0$, the capillary radii are uniformly distributed between $r_{\min}$ and $r_{\max}$. When m increases, the pore distribution becomes skewed towards smaller capillary radii as demonstrated in Fig. 2. Many natural geological media follow the SSPSD [19]. We assume that the REV is initially fully saturated and then drained when it is subjected to a pressure head h (m). For a capillary tube, the pore radius r_h (m) is related to h via the Young-Laplace equation [24]

$$h = \frac{2T_s cos\beta}{\rho_w g r_h}, \qquad (2.2)$$

where T_s (N/m) is the interface tension and β (^{o}) is contact angle between the solid walls and saturating immiscible fluid phases. Under the pressure head h, the capillary becomes completely desaturated if its radius r is larger than r_h given by Eq. (2.2). If the medium is at capillary pressure equilibrium, all capillaries with radii $r > r_h$ are to be saturated by the non-wetting phase (i.e., air) and those with radii $r \le r_h$ are to be saturated by the wetting phase (i.e., water). The effective water saturation $S_{\mathrm{we}}(h)$ is computed from the PSD as [21]:

$$\begin{aligned} S_{\mathrm{we}}(h) &= \frac{\int_{r_{\min}}^{r_h} \pi r^2 L_\tau f(r)\mathrm{d}r}{\int_{r_{\min}}^{r_{\max}} \pi r^2 L_\tau f(r)\mathrm{d}r} \\ &= \frac{\int_{r_{\min}}^{r_h} r^2 f(r)\mathrm{d}r}{\int_{r_{\min}}^{r_{\max}} r^2 f(r)\mathrm{d}r}, \end{aligned} \qquad (2.3)$$

where L_τ is the tortuous length of capillaries and that is considered invariant over all capillaries of the REV (Fig. 1). The length L_τ is always greater than the length L_o of the REV and related to L_o by

$$L_\tau = \tau L_o, \qquad (2.4)$$

where τ is defined as the mean tortuosity of porous media. Combining Eqs. (2.1)-(2.3), the following is obtained:

$$S_{\mathrm{we}} = \frac{(r_h - r_{\min})}{(r_{\max} - r_{\min})} \qquad (2.5)$$

$$\times \frac{\left[2r_h^2 + 2r_{\min}r_h(1+m) + r_{\min}^2(1+m)(2+m)\right]}{\left[2r_{\max}^2 + 2r_{\min}r_{\max}(1+m) + r_{\min}^2(1+m)(2+m)\right]}.$$

The porosity of the REV is defined as [22, 23]

$$\begin{aligned} \phi &= \frac{\int_{r_{\min}}^{r_{\max}} \pi r^2 L_\tau f(r)\mathrm{d}r}{A_{\mathrm{REV}} L_o} \\ &= \frac{\tau \int_{r_{\min}}^{r_{\max}} \pi r^2 f(r)\mathrm{d}r}{A_{\mathrm{REV}}}, \end{aligned} \qquad (2.6)$$

where A_{REV} is the cross sectional area that is perpendicular to the flow direction (Fig. 1).

If a capillary with the radius r and the length L_τ is filled with water, its resistance (R) is given by [22, 23]:

$$\frac{1}{R(r)} = \frac{\pi r^2 \sigma_w}{L_\tau} + \frac{2\pi r \Sigma_s}{L_\tau}, \qquad (2.7)$$

where σ_w (S/m) is the electrical conductivity of water and Σ_s (S) is the specific surface conductance at the interface between water and the capillary wall.

The resistance of the REV under partially saturated conditions is the sum of resistances of water-filled capillaries (resistances in parallel) as

$$\begin{aligned}\frac{1}{R_o} &= \int_{r_{\min}}^{r_h} \frac{1}{R(r)} f(r)\mathrm{d}r \\ &= \int_{r_{\min}}^{r_h} \frac{\pi r^2 \sigma_w}{L_\tau} f(r)\mathrm{d}r \\ &+ \int_{r_{\min}}^{r_h} \frac{2\pi r \Sigma_s}{L_\tau} f(r)\mathrm{d}r. \end{aligned} \qquad (2.8)$$

According to definition, the electrical conductivity of the REV is related to its resistance as

$$\sigma = \frac{L_o}{R_o A_{\mathrm{REV}}}. \qquad (2.9)$$

Combining Eqs. (2.4)-(2.9), one obtains a general expression for σ as

$$\begin{aligned}\sigma =& \frac{\phi \sigma_w}{\tau^2} \frac{\int_{r_{\min}}^{r_h} r^2 f(r)\mathrm{d}r}{\int_{r_{\min}}^{r_{\max}} r^2 f(r)\mathrm{d}r} \\ &+ \frac{2\phi \Sigma_s}{\tau^2} \frac{\int_{r_{\min}}^{r_h} r f(r)\mathrm{d}r}{\int_{r_{\min}}^{r_{\max}} r^2 f(r)\mathrm{d}r}. \end{aligned} \qquad (2.10)$$

From Eqs. (2.3)-(2.10), we can express σ in terms of the effective water saturation as

$$\begin{aligned}\sigma =& \frac{\phi \sigma_w}{\tau^2} S_{\mathrm{we}} \\ &+ \frac{2\phi \Sigma_s S_{\mathrm{we}}}{\tau^2} \frac{\int_{r_{\min}}^{r_h} r f(r)\mathrm{d}r}{\int_{r_{\min}}^{r_h} r^2 f(r)\mathrm{d}r} \end{aligned} \qquad (2.11)$$

Eq. (2.11) can be applied for any kind of PSD in porous media (e.g., fractal, lognormal or double lognormal). For a specific SSPSD given by Eq□. (2.1)-(2.11) can be written as

$$\begin{aligned}\sigma =& \frac{\phi S_{\mathrm{we}}}{\tau^2}\Big(\sigma_w + 2\Sigma_s \times \\ & \frac{r_h(3+m) + 2r_{\min}(1+m)(3+m)}{2r_h^2 + 2r_{\min} r_h (1+m) + r_{\min}^2 (1+m)(2+m)}\Big). \end{aligned} \qquad (2.12)$$

Eq. (2.12) is the key finding of this work. It indicates that the electrical conductivity of partially saturated porous media depends on effective water saturation S_{we} (i.e., r_h), electrical conductivity of pore water σ_w, specific surface conductance Σ_s and the microstructural parameters (ϕ, $r_{\min}$, $r_{\max}$ and m). The first and second terms in Eq. (2.12) are conductivity contributions from pore water and interface between water and solid mineral surface, respectively. From Eq. (2.12), one can investigate the dependence of the electrical conductivity on the saturation state of porous media. We remark that under fully saturated conditions, that is $S_{\mathrm{we}} = 1$ and $r_h = r_{\max}$, Eq. (2.12) reduces to the result proposed in [22].

It should be noted that for the fractal PSD in which $f(r)$ is given by [21]

$$f(r) = D_f r_{\max}^{D_f} r^{-D_f - 1}, \qquad (2.13)$$

where D_f is the fractal dimension for pore space ($1 < D_f < 2$), one can readily obtain an expression for the electrical conductivity of porous media σ using the same approach as performed to obtain Eq. (2.12) for the SSPSD as

$$\sigma = \frac{\phi S_{\mathrm{we}}}{\tau^2}\left(\sigma_w + 2\Sigma_s \frac{2-D_f}{1-D_f} \frac{r_h^{1-D_f} - r_{\min}^{1-D_f}}{r_h^{2-D_f} - r_{\min}^{2-D_f}}\right). \qquad (2.14)$$

From Eqs. (2.12)-(2.14), we can find that when the electrical surface conductivity is negligible, that is $\Sigma_s = 0$, the electrical conductivity σ is independent of the PSD of porous media. In other words, Eq. (2.12) for the SSPSD is identical to Eq. (2.14) for the fractal PSD when the surface conductivity is negligible.

The form of Eq. (2.12) or Eq. (2.14) is similar to classical models reported in literature [13,25–27]. For example, Linde and co-authors obtained the following expression [28]:

$$\sigma = \phi^p \left[\sigma_w S_w^n + (\phi^p - 1)\sigma_s\right], \quad (2.15)$$

where S_w (unitless) is water saturation, p is the cementation exponent and n is the Archie′ second exponent and σ_s is the surface conductivity.

We remark that a capillary bundle model used for our proposed model assumes that porous media are conceptualized as a bundle of parallel capillary tubes without intersections between them. Therefore, the model is not meant to be a perfect representation of the pore space in most geologic porous media. However, to the best of our knowledge, the capillary bundle model has been effectively used to provide useful insight and explanation into transport phenomena in porous media with a long history [14–18].

3. Results and Discussion

3.1 Sensitivity analysis of the model

Firstly, we numerically solve Eq. (2.12) to obtain the dependence of σ on the effective saturation for a representative porous medium (e.g., $\phi = 0.3$, $\tau = 1.2$, $r_{\min} = 10^{-7}$ m, $r_{\max} = 10^{-4}$ m, $\sigma_w = 10^{-4}$ S/m and $\Sigma_s = 10^{-9}$ S) for three values of m (m = 5, 15 and 30) as shown in Fig. 3. It is noted that, in Eq. (2.12), we obtain

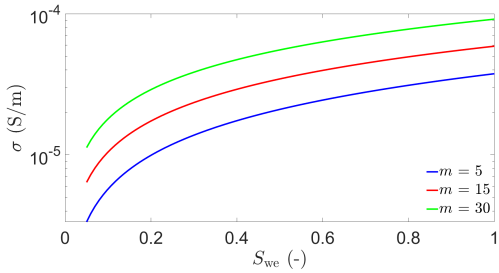

Fig. 3. The EC of porous media as a function of S_{we} for a representative porous medium (e.g., $\phi = 0.3$, $\tau = 1.2$, $r_{\min} = 10^{-7}$ m, $r_{\max} = 10^{-4}$ m, $\sigma_w = 10^{-4}$ S/m and $\Sigma_s = 10^{-9}$ S) for three values of m (m = 5, 15 and 30).

r_h from corresponding values of S_{we} using Eq. (2.5). The result shows that σ increases with increasing effective saturation as observed in literature regardless of values of m [10, 29]. Additionally, σ is very sensitive with m, that is the PSD of the porous medium. Namely, for a given value of S_{we}, the EC increases with increasing m. This is attributed to the fact that when m increases, the pore distribution becomes skewed towards smaller capillary radii or there are a larger number of small pores. As shown by Eq. (2.7), the surface conductivity of a single water-filled capillary is larger for smaller radii. Consequently, the surface conductivity and, hence, the total EC of porous media increase with increasing m at the same value of S_{we}. To indicate the influence of the electrical surface conductance Σ_s on the EC of porous media, we show variation of σ with σ_w for a representative porous medium (e.g., $\phi = 0.3$, $\tau = 1.2$, $r_{\min} = 10^{-7}$ m, $r_{\max} = 10^{-4}$ m, $m = 30$) at fully saturation conditions (i.e., $S_{we} = 1$ and $r_h = r_{\max}$) for three values of Σ_s (1×10^{-9} S, 20×10^{-9} S and 50×10^{-9} S) using Eq. (2.12) (see Fig. 4). It is seen that σ increases with increasing σ_w as expected [25,29]. Additionally, Σ_s only plays an important role for small values of σ_w. There-

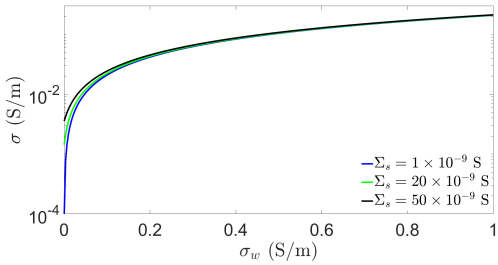

Fig. 4. The EC porous media as a function of σ_w for a representative porous medium (e.g., $\phi = 0.3$, $\tau = 1.2$, $r_{\min} = 10^{-7}$ m, $r_{\max} = 10^{-4}$ m, $m = 30$) for three values of Σ_s (1×10^{-9} S, 20×10^{-9} S and 50×10^{-9} S).

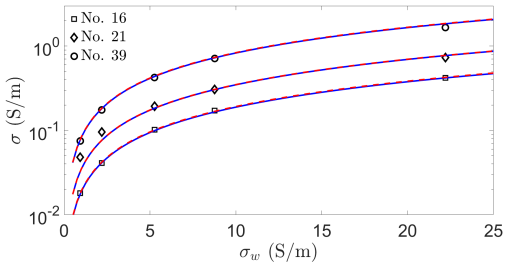

Fig. 5. Dependence of σ on σ_w for fully saturated porous media reported by [25] for three samples (sample numbers: 16, 21, 39) of shaly sandstone (symbols). The blue solid lines are predicted from the proposed model, Eq. (2.12), with $S_{\text{we}} = 1$ and $r_h = r_{\max}$. The red dashed lines are predicted from Archie′law [29], that is a special case of Eq. (2.15) with $S_w = 1$ and $\sigma_s = 0$. Parameter values entering the model are listed in Table 1.

fore, one can neglect the surface conductivity when σ_w is larger than 0.5 S/m for natural geological media in which pore sizes are typically in μm as reported in literature [30, 31].

3.2 Comparison with experimental data

Fig. 5 shows the dependence of σ on σ_w under fully saturated conditions for three samples (sample numbers: 16, 21, 39) of shaly sandstone reported by [25] (see symbols). As shown in Fig. 5, the range of σ_w used by [25] is larger than 0.5 S/m, we can safely ignore the surface conductivity ($\Sigma_s = 0$) as previously discussed. Therefore, we are able to explain the observed behavior using Eq. (2.12) or Eq. (2.14) with $S_{\text{we}} = 1$ and $r_h = r_{\max}$. Parameter values entering the model (ϕ, τ, $r_{\min}$, $r_{\max}$) for each sample are listed in Table 1. It is noted that we take values of ϕ, $r_{\min}$ and $r_{\max}$ from [23] for the same samples. For values of τ and m, we empirically find those so that the model is capable of providing a relatively good fit with experimental data. Values of τ between to 1.6 and 2.5 are in good agreement with those reported by [32] for similar samples. The prediction from the proposed model is shown by blue solid lines for each sample. Additionally, we apply the Archie′law [29] under fully saturated condition, that is $\sigma = \sigma_w \phi^p$ (special case of Eq. (2.15) with $S_w = 1$ and $\sigma_s = 0$) to reproduce the measured data (red dashed lines). Values of p entering the Archie′law for each sample are empirically found and listed in Table 1. The comparison shows that that the model prediction is in very good agreement with the measured data reported by [25] and with the one predicted by the Archie′law.

Fig. 6 shows variation of σ with S_{we} that we deduce from experimental data reported by [33] (see symbols) for two samples of Plaggen soil (sample PS11 and PS13) at two different values of σ_w (σ_w = 1.34 S/m for PS11 and σ_w = 2.25 S/m for PS13). To deduce S_{we} from water content θ that was reported in [33] for each sample, we use the following relation [21, 23]:

$$S_{\text{we}} = \frac{\theta - \theta_r}{\phi - \theta_r}, \tag{3.1}$$

where θ_r is irreducible water content. Eq. (3.1) can be written in terms of water satu-

Table 1. Values of parameters entering the model, Eq. (2.12) with $S_{\rm we} = 1$ and $r_h = r_{\rm max}$ and entering the Archie'law [29], that is a special case of Eq. (2.15) with $S_w = 1$ and $\sigma_s = 0$ for comparison with experimental data reported by [25] for the case of fully saturated conditions. The asterisk symbol * stands for reported values in corresponding reference.

No.	ϕ^* (-)	τ (-)	$r_{\rm min}$ (μm)	$r_{\rm max}$ (μm)	Σ_s (S)	m (-)	p (-)
16	0.12	2.5	0.032	32	0	5	1.85
31	0.14	2	0.026	2.6	0	5	1.7
29	0.21	1.6	0.025	25	0	5	1.6

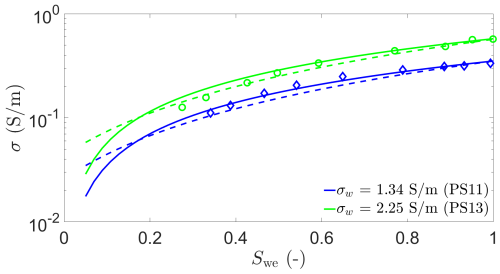

Fig. 6. Variation of σ with $S_{\rm we}$ that we deduce from experimental data reported by [33] for two samples of Plaggen soil at two different values of σ_w (symbols). The solid lines and dashed lines are, respectively, predicted from the proposed model given by Eq. (3.3) and the one given by Eq. (2.15) when neglecting the surface conductivity (i.e., $\sigma_s = 0$).

ration S_w as

$$S_{\rm we} = \frac{S_w - S_r}{1 - S_r}, \qquad (3.2)$$

where $S_w = \theta/\phi$ and $S_r = \theta_r/\phi$.

Since values of σ_w (1.34 S/m and 2.25 S/m) used by [33] are large, we can neglect the surface conductivity as mentioned earlier in sub-section 3.1. Therefore, Eq. (2.12) reduces to

$$\sigma = \frac{\phi S_{\rm we}}{\tau^2}\sigma_w. \qquad (3.3)$$

Using Eq. (3.3), we can reproduce experimental data given by [33] (see solid lines). Values of ϕ for each sample were reported by [33] and are re-shown in Table 2. We empirically find values for τ and θ_r so that the model is in relatively good agreement with experimental data. Found values for τ and θ_r are shown in Table 2. Additionally, we can explain the observed behavior in Fig. 6 using the model given by [28], Eq. (2.15), with $p = 1.5$ and $n = 1.6$ which are empirically searched when neglecting the surface conductivity (i.e., $\sigma_s = 0$) as shown by dashed lines. Note that values of p and n are in good agreement with published results [27, 34]. It is shown that the proposed model is well able to reproduce experimental data reported by [25] and in good match with the model given by [28].

Similarly, Fig. 7 shows variation of σ with $S_{\rm we}$ for loam soil reported by [35] (symbols) at $\sigma_w = 7.2\times10^{-2}$ S/m and the model prediction from Eq. (2.12) (solid line). Parameters τ, $r_{\rm min}$, $r_{\rm max}$, Σ_s, m and θ_r are not yet available in [35]. Therefore, we empirically find them so that the model is in relatively good agreement with experimental data. Their optimized values are shown in Table 2. Note that values of Σ_s are in agreement with reported ones in literature (e.g., $\Sigma_s = 8.9\times10^{-9}$ S by [36] or 1.4×10^{-9} by [37]). It is shown that the model is well capable of reproducing experimental data reported by [35].

Table 2. Values of parameters entering the model, Eq. (3.3) or Eq. (2.12), for comparison with experimental data reported by [33] and [35]. The asterisk symbol * stands for reported values in corresponding reference.

ID	ϕ^* (-)	τ (-)	$r_{\min}$ (μm)	$r_{\max}$ (μm)	Σ_s (S)	m (-)	θ_r (-)	ref ref
PS11	0.413	1.25	-	-	-	-	0.08	[33]
PS13	0.410	1.25	-	-	-	-	0.08	[33]
Loam	0.44	1.2	0.032	32	20.10^{-9}	60	0.01	[35]

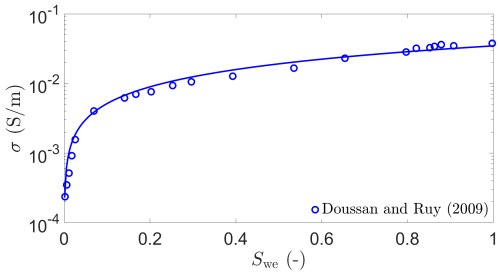

Fig. 7. Variation of σ with $S_{\rm we}$ for loam soil reported by [35] (symbols) at $\sigma_w = 7.2\times10^{-2}$ S/m. The solid line is predicted from the proposed model, Eq. (2.12), with model parameters listed in Table 2.

4. Conclusions

We develop an EC model for porous media under partially saturated conditions using a bundle of capillary tubes model that follows the similarly skewed PSD. The proposed model is expressed in terms of electrical conductivity of the pore water (σ_w), electrical surface conductivity (Σ_s), water saturation ($S_{\rm we}$), mirostructure parameters of porous media (e.g., ϕ, τ, $r_{\min}$ and $r_{\max}$) and pore size distribution of media (e.g., m). The obtained model is then numerically analyzed and successfully compared with published experimental data and published models. Lastly, we remark that the proposed approach can apply for any pore size distribution of porous media such as fractal, lognormal or double lognormal distribution. Along with other EC models in available literature, this new physically-based model may pave the way for characterizing hydrological processes with EC measurements. In the future, we will extend this work with consideration of hysteresis effects.

Acknowledgments

This research is funded by Vietnam National Foundation for Science and Technology Development (NAFOSTED) under grant number 103.99-2023.04

References

[1] Binley A, Hubbard SS, Huisman JA, Revil A, Robinson DA, Singha K, et al. The emergence of hydrogeophysics for improved understanding of subsurface processes over multiple scales. Water Resources Research. 2015;51(6):3837-66.

[2] Loiseau B, Carrière SD, Jougnot D, Singha K, Mary B, Delpierre N, et al. The geophysical toolbox applied to forest ecosystems–A review. Science of the Total Environment. 2023:165503.

[3] Kemna A, Vanderborght J, Kulessa B, Vereecken H. Imaging and characterization of subsurface solute transport using electrical resistivity tomography (ERT) and equivalent transport models. Journal of hydrology. 2002;267(3-4):125-46.

[4] Samouëlian A, Cousin I, Tabbagh A, A B, Richard G. Electrical resistivity survey in soil science: A review. Soil and Tillage Research. 2005 09;83:173-93.

[5] Archie GE. The electrical resistivity log as an aid in determining some reservoir characteristics. Petroleum Transactions of AIME. 1942;146:54-62.

[6] Friedman SP. Soil properties influencing apparent electrical conductivity: a review. Computers and Electronics in Agriculture. 2005;46(1):45-70.

[7] Laloy E, Javaux M, Vanclooster M, Roisin C, Bielders CL. Electrical Resistivity in a Loamy Soil: Identification of the Appropriate Pedo-Electrical Model. Vadose Zone Journal. 2011;10:1023-33.

[8] Ewing RP, Hunt AG. Dependence of the Electrical Conductivity on Saturation in Real Porous Media. Vadose Zone Journal. 2006;5(2):731-41.

[9] Cai J, Wei W, Hu X, Wood DA. Electrical conductivity models in saturated porous media: A review. Earth Science Reviews. 2017;171:419-33.

[10] Sen PN, Scala C, Cohen MH. A self□similar model for sedimentary rocks with application to the dielectric constant of fused glass beads. Geophysics. 1981;46(5):781-95.

[11] Wang KW, Sun JM, Guan JT, Zhu DW. A percolation study of electrical properties of reservoir rocks. Physica A: Statistical Mechanics and its Applications. 2007;380:19 26.

[12] Mualem Y, Friedman SP. Theoretical Prediction of Electrical Conductivity in Saturated and Unsaturated Soil. Water Resources Research. 1991;27(10):2771-7.

[13] Waxman MH, Smits LJM. Electrical conductivities in oil bearing shaly sands. Society of Petroleum Engineers Journal. 1968;8:107-22.

[14] Brovelli A, Cassiani G, Dalla E, Bergamini F, Pitea D, Binley AM. Electrical properties of partially saturated sandstones: Novel computational approach with hydrogeophysical applications. Water Resources Research. 2005;41(8).

[15] Bussian AE. Electrical conductance in a porous medium. Geophysics. 1983;48(9):1258-68.

[16] Ghanbarian B, Hunt A, Skinner T, Ewing RP. Saturation dependence of transport in porous media predicted by percolation and effective medium theories. Fractals. 2015;23(01):1540004.

[17] Pride S. Governing equations for the coupled electromagnetics and acoustics of porous media. Physical Review B. 1994;50(21):15678-96.

[18] Linde N, Binley A, Tryggvason A, Pedersen LB, Revil A. Improved hydrogeophysical characterization using joint inversion of cross-hole electrical resistance and ground-penetrating radar traveltime data. Water Resources Research. 2006;42(12).

[19] Thanh LD, Jougnot D, Van Do P, Van Nghia A N. A physically based model for the electrical conductivity of watersaturated porous media. Geophysical Journal International. 2019;219(2):866-76.

[20] Rembert F, Jougnot D, Guarracino L. A fractal model for the electrical conductivity of water-saturated porous media during mineral precipitation-dissolution processes. Advances in Water Resources. 2020;145:103742.

[21] Luo H, Jougnot D, Jost A, Teng J, Thanh LD. A capillary bundle model for the electrical conductivity of saturated frozen porous media. Journal of Geophysical Research: Solid Earth. 2023;128(3):e2022JB025254.

[22] Soldi M, Rembert F, Guarracino L, Jougnot D. Electrical conductivity model

for reactive porous media under partially saturated conditions with hysteresis effects. Advances in Water Resources. 2024;193:104815.

[23] Luo H, Jougnot D, Jost A, Teng J, Mendieta A, Lin G, et al. Predicting the electrical conductivity of partially saturated frozen porous media, a fractal model for wide ranges of temperature and salinity. Water Resources Research. 2024;60(3):e2023WR034845.

[24] Jackson MD. Multiphase electrokinetic coupling: Insights into the impact of fluid and charge distribution at the pore scale from a bundle of capillary tubes model. Journal of Geophysical Research: Solid Earth. 2010;115(B7).

[25] Vinogradov J, Hill R, Jougnot D. Influence of pore size distribution on the electrokinetic coupling coefficient in two-phase flow conditions. Water. 2021;13(17):2316.

[26] Solazzi SG, Thanh LD, Hu K, Jougnot D. Modeling the Frequency-Dependent Effective Excess Charge Density in Partially Saturated Porous Media. Journal of Geophysical Research: Solid Earth. 2022;127(11):e2022JB024994.

[27] Nghia NV, Hung N, Thanh L. A Model for Electrical Conductivity of Porous Materials under Saturated Conditions. VNU Journal of Science: Mathematics - Physics. 2021;37(2).

[28] Thanh LD, Jougnot D, Van Do P, Tuyen VP, Ca NX, Hien NT. A physically based model for the electrical conductivity of partially saturated porous media. Geophysical Journal International. 2020;223(2):993-1006.

[29] Jurin J. II. An account of some experiments shown before the Royal Society; with an enquiry into the cause of the ascent and suspension of water in capillary tubes. Philosophical Transactions of the Royal Society of London. 1719;30(355):739-47.

[30] Revil A, Cathles III LM, Losh S, Nunn JA. Electrical conductivity in shaly sands with geophysical applications. Journal of Geophysical Research: Solid Earth. 1998;103(B10):23925-36.

[31] Glover P. What is the cementation exponent? A new interpretation. The Leading Edge. 2009;28(1):82-5.

[32] Alkafeef SF, Alajmi AF. Streaming potentials and conductivities of reservoir rock cores in aqueous and non-aqueous liquids. Colloids and Surfaces A: Physicochem Eng Aspects. 2006;289:141-8.

[33] Thanh LD, Sprik R. Permeability dependence of streaming potential coefficient in porous media. Geophysical Prospecting. 2016;64(3):714-25.

[34] Nishiyama N, Yokoyama T. Permeability of porous media: Role of the critical pore size. Journal of Geophysical Research: Solid Earth. 2017;122(9):6955-71.

[35] Weerts AH, Bouten W, Verstraten JM. Simultaneous measurement of water retention and electrical conductivity in soils: Testing the Mualem-Friedman Tortuosity Model. Water Resources Research. 1999;35(6):1781-7.

[36] Berg CF, Kennedy WD, Herrick DC. Conductivity in partially saturated porous media described by porosity, electrolyte saturation and saturation-dependent tortuosity and constriction factor. Geophysical Prospecting. 2022;70(2):400-20.

[37] Doussan C, Ruy S. Prediction of unsaturated soil hydraulic conductivity with electrical conductivity. Water Resources Research. 2009;45(10).

[38] Revil A, Glover PWJ. Nature of surface electrical conductivity in natural sands,

sandstones, and clays. Geophysical Research Letters. 1998;25(5):691-4.

[39] Lorne B, Perrier F, Avouac JP. Streaming potential measurements: 1. Properties of the electrical double layer from crushed rock samples. Journal of Geophysical Research. 1999;104(B8):17.857-17.877.